JOURNAL OF TISSUE ENGINEERING AND REGENERATIVE MEDICINE
J Tissue Eng Regen Med (2011).
Published online in Wiley Online Library (wileyonlinelibrary.com) **DOI:** 10.1002/term.394

RESEARCH ARTICLE

Development of an osteoconductive PCL–PDIPF–hydroxyapatite composite scaffold for bone tissue engineering

Juan Manuel Fernandez[1,2], M. Silvina Molinuevo[1], M. Susana Cortizo[2] and Ana M. Cortizo[1]*
[1]*Grupo de Investigación en Osteopatías y Metabolismo Mineral (GIOMM), Departamento de Ciencias Biológicas, Facultad de Ciencias Exactas, Universidad Nacional de La Plata, 1900 La Plata, Argentina*
[2]*Instituto de Investigaciones Fisicoquímica Teóricas y Aplicadas (INIFTA), Facultad de Ciencias Exactas, Universidad Nacional de La Plata, 1900 La Plata, Argentina*

Abstract

Hydroxyapatite (HAP)-containing poly-ε-caprolactone (PCL)–polydiisopropyl fumarate (PDIPF) composite (Blend) was developed as an alternative for bone tissue engineering. The physicochemical, mechanical and biocompatibility properties of these composites were evaluated using two osteoblast-like cell lines (UMR106 and MC3T3E1) and compared with the blend without HAP and PCL/HAP films. The increment in the elastic modulus and the decrease in the elongation-at-break of Blend–HAP suggest that the mechanical properties of the HAP scaffolds have improved significantly. The addition of HAP to both PCL and Blend significantly improves the cell biocompatibility and osteogenicity of the scaffolds. Evidence for this notion is based in several observations: (a) HAP–polymer increases proliferation of osteoblastic cells; (b) HAP included in the blend increases the ALP expression in UMR106 cells; (c) HAP–Blend increases the type-I collagen production in both cell lines, and d) higher levels of the osteogenic transcription factor Runx-2 were detected when MC3T3E1 osteoblasts were induced to differentiate and mineralize on HAP–polymer scaffolds. In conclusion, a novel biocompatible HAP–Blend composite with uniform dispersion of semi-nano HAP particles and good interphase compatibility has been prepared successfully. The development of HAP–Blend composite, with improved physical, mechanical and osteoinductive properties, may potentially be used in bone tissue-engineering applications. Copyright © 2011 John Wiley & Sons, Ltd.

Received 28 July 2010; Accepted 11 November 2010

Keywords bone tissue engineering; biocompatibility; poly-ε-caprolactone; polydialkyl fumarates; hydroxyapatite; osteoblasts

1. Introduction

Tissue-engineering strategies have led to the development of artificial scaffolds, which can simulate biological extracellular matrix, supporting adhesion, proliferation, differentiation and tissue regeneration (Mano *et al*., 2007). Different synthetic or natural polymers have been used to fabricate matrix for bone regeneration, such as polyesters (polyglycolide, polylactides) and poly-ε-caprolactones and their copolymers (Habibovic and de Groot, 2007). These materials are characteristically hydrolytically degradable and biocompatible, although they do not show good mechanical properties. Thus, no single polymer has been found to meet all the requirements needed for a bone scaffold.

In previous studies, we have used polyester (poly-β-propiolactone, PBPL; poly-ε-caprolactone, PCL) and poly-fumarate (polydiisopropyl fumarate, PDIPF; polydicyclohexyl fumarate, PDCF) mixtures to create scaffolds which support *in vitro* osteoblastic development (Cortizo *et al*.,

**Correspondence to: Ana M. Cortizo, GIOMM, Departamento de Ciencias Biológicas, Facultad de Ciencias Exactas, UNLP, 47 y 115 (1900) La Plata, Argentina.*
E-mail: cortizo@biol.unlp.edu.ar

2008). Our studies have shown that polyester–PDIPF matrices (Cortizo *et al*., 2008) as well as PCL–PDIPF blends (Fernandez *et al*., 2010) support adhesion, proliferation and differentiation of UMR106 and MC3T3E1 osteoblastic cell lines without evidence of cytotoxicity. In addition we investigated the degradation capabilities of the different films. Under acellular conditions, only PBPL was hydrolytically degraded. However, macrophages cultured on PDIPF films demonstrated a significant degradation of polymers, indicating that polyfumarates as well as polyesters can be degraded by cellular mechanisms (Cortizo *et al*., 2008).

The mechanical properties of polymeric materials can be improved by the addition of calcium phosphate bioceramics. For instance, hydroxyapatite (HAP) and tricalcium phosphate have been widely used to create composite scaffolds for bone tissue regeneration (Kim *et al*., 2006; Wang, 2003). The inclusion of these materials in polymeric scaffolds makes them more brittle, limited for modelling and with a longer degradation rate (Wang, 2003). The idea is to find a material that can be modelled and can simulate the mechanical and biological properties of an implant. In actual fact, bone tissue is a composite of nano-hydroxyapatite crystals immersed in a collagen and non-collagen protein matrix.

One important step in the development of scaffolds for tissue engineering is to evaluate the biocompatibility and cytotoxicity of the materials (Salgado *et al*., 2004). These studies are based on the morphological and biochemical changes of cells, growth and cell differentiation. The success of the construct will depend on the ability of the scaffold to induce the development of osteoblast and bone transcription factors outside of the body or by stimulating cells to migrate into the implant. In the present study, we fabricated HAP–PCL and HAP–PCL–PDIPF composite scaffolds through a simple solution-based chemical method which provides a very good dispersion of HAP particles in the matrix polymer, yielding a composite with an uniform structure. We have analysed the physicochemical, mechanical and biocompatibility properties of these composites for future applications in bone tissue engineering.

2. Materials and methods

2.1. Synthesis and characterization of composite scaffolds

Poly-ε-caprolactone (PCL) was purchased from Aldrich and has a weight average molecular weight (MW) and polydispersity index of 65 000 g/M and 1.4, respectively, as indicated by the manufacturer. Poly(di-isopropylfumarate) (PDIPF) was synthesized by microwave-assisted radical polymerization, using benzoyl peroxide as the initiator (Cortizo, 2007). The weight average molecular weight and polydispersity index were 131 000 g/M and 2.0, respectively, determined by size exclusion chromatography (SEC).

Compatibilized blends of PCL and PDIPF (75:25 wt%; Blend) were obtained by ultrasound using Bandelin HD60 equipment at 20 °C, as previously described (Fernandez *et al*., 2010).

Hydroxyapatite (HAP) was obtained as follows. Adult bovine femur was procured from a local slaughterhouse and cleaned to remove visible soft tissues on the bone surface. It was then cut into small samples. The samples were first incinerated with a burner and then with an electric furnace (in order to eliminate organic materials), under normal atmosphere conditions, at 900 °C, using a heating rate of 5 °C/min with 2 h holding time (Ooi *et al*., 2007). The ashes were crushed and sifted (number 200, pore size 75 μm) and subsequently processed by ultrasound until a size of approximately 200 nm was attained.

Composites of 1 wt% HAP and PCL or Blend were obtained by dissolution in chloroform and casting in a glass Petri dish. The solvent was allowed to evaporate at room temperature and then the resulting films were dried under vacuum until constant weight. The films were sterilized by UV exposure for 2 h (Fernandez *et al*., 2010).

The weight average molecular and molecular weight distribution of the polymers were determined by size exclusion chromatography, using an LKB-2249 instrument at 25 °C. A series of μ-Styragel columns, pore sizes 10^5, 10^4, 500 and 100 Å, were used with chloroform as an eluent. The polymer concentration was 4–5 mg/ml and the flow rate was 0.5 ml/min. The polymer was detected at 5.75 μm with a Miran 1A infrared spectrophotometer detector and calibration was performed using poly(methyl methacrylate) as standard.

The surface roughness of the HAP and of the composites was investigated using scanning electron microscopy (SEM; Phillips 505, The Netherlands), with an accelerating voltage of 20 kV. The images were analysed by Soft Imaging System ADDAII. In addition, Ca:P ratio of the HAP was evaluated by SEM coupled with an energy-dispersive X-ray (EDX) analysis detector.

FTIR spectra of HAP and Blend–HAP were recorded on a Nicolet 380 FTIR between 4000–400 cm^{-1} with a resolution of 4 cm^{-1} and 32 scans of accumulation. EZ-OMNIC software was used to analyse the spectra.

The tensile properties of the composites were determined with a universal testing machine (Digimess TC500), using force load cell ('Interface' of Arizona, USA), SM-50 N capacity, at room temperature. The dog bone-shaped specimens (50 × 18 mm^2) were tested at a rate of 5 mm/min until breaking point. Ultimate tensile stress, elastic modulus and elongation at breaking point were calculated on the basis of the generated tensile stress–strain curves. The results presented are the mean values of eight independent measurements.

HAP particle distribution within the films was investigated by staining with alizarin red S. Images were recorded using an Eclipse E400 Nikon microscope and a Nikon Coolpix 4500 digital camera.

DOI: 10.1002/term

2.2. Biocompatibility studies

2.2.1. Cell cultures and incubations

UMR106 rat osteosarcoma cells or MC3T3E1 mouse calvaria-derived cells were grown in Dulbecco's modified Eagle's medium (DMEM) containing 10% FBS, 100 U/ml penicillin and 100 μg/ml streptomycin at 37 °C in a 5% CO_2 atmosphere (McCarthy *et al*., 1997). The cells were seeded in standard tissue culture flasks and subcultured using trypsin–EDTA. The UMR106 cell line has been shown to conserve certain characteristics of differentiated osteoblastic phenotype (Partridge *et al*., 1983). In the case of non-transformed MC3T3E1 cells, previous studies have demonstrated that expression of osteoblastic markers begins after culturing the cells with medium supplemented by 5 mM β-glycerol-phosphate (βGP) and 25 μg/ml ascorbic acid (AA) (Quarles *et al*., 1992). Under these culture conditions, alkaline phosphatase activity (ALP) begins to be expressed after 1 week and reaches a maximum after 2 weeks, while mineralization is achieved after extending the culture to 3 weeks. However, the cells only undergo active replication during the first 5 days of incubation. For the different experiments, 0.8 mm diameter composite scaffolds were placed in 24-well plates and sterilized by UV. Then the cells were seeded onto 10% FBS–DMEM-presoaked scaffolds and incubated during the periods of time indicated in the legends to the figures.

2.2.2. Evaluation of osteoblastic growth and differentiation

The ability of osteoblastic cells to grow and express markers of differentiation associated with bone-forming capacity was evaluated by measurement of the number of cells stained with haematoxylin and eosin (H&E 48 h culture), alkaline phosphatase (ALP) activity and collagen production (Fernandez *et al*., 2010; Cortizo *et al*., 2006). Briefly, cells were fixed with methanol for 5 min and then stained with H&E for 10 min, after which cell proliferation was evaluated by counting the number of cells/field in 10 fields per experimental condition. For ALP determination, cells were washed with phosphate-buffered saline (PBS) and solubilized in 0.5 ml 0.1% Triton X-100. Aliquots of this total cell extract were used for protein determination by the Bradford (1976) technique, and for measurement of ALP by spectrophotometric determination of initial rates of hydrolysis of *p*-nitrophenyl-phosphate (p-NPP) to *p*-nitrophenol (p-NP) at 37 °C for 10 min. For type I collagen production, cells were fixed with Bouin's solution and stained with Sirius red dye for 1 h. The stained material was dissolved in 1 ml 0.1 N sodium hydroxide and the absorbance of the solution was recorded at 550 nm (Tullberg-Reinert and Jundt, 1999).

2.3. Transcription factor Runx and Osteocalcin expression by western blot analysis

MC3T3E1 were grown for different incubation periods onto scaffolds in DMEM–10% FBS and then differentiated into osteoblasts as described above. At the end of different culture periods, cells were lysed in Laemmli's buffer (Laemmli, 1970). These lysates were heated to 100 °C for 3 min, and 30 μg protein subjected to 12% SDS–PAGE. The separated proteins were then transferred to PVDF membranes. After washing and blocking, the membranes were incubated overnight at 4 °C with an antibody directed against Cbfa-1/Runx-2 (Santa Cruz Biotechnology, Santa Cruz, CA, USA) for evaluation of osteoblastogenesis (Molinuevo *et al*., 2010). In order to normalize the results, all blots were stripped and reprobed with an anti-β-actin antibody (Sigma, St. Louis, MO, USA). Blots were developed by an enhanced chemiluminescence method. The intensity of the specific bands was quantified by densitometry after scanning of the photographic film. Images were analysed using the Scion-β2 program.

2.4. Statistical analysis

Results are expressed as the mean ± SEM and, unless indicated otherwise, were obtained from two separate experiments performed in triplicate. Differences between the groups were assessed by one-way ANOVA with Tukey *post hoc* test. For non-Normal distributed data, non-parametrical Kruskal–Wallis with Dunn *post hoc* test was performed, using GraphPad InStat v. 3.00 (Graph Pad Software, San Diego, CA, USA). $p < 0.05$ was considered significant for all statistical analyses.

3. Results

3.1. Characterization of HAP, PCL–HAP and Blend–HAP composite scaffolds

Since a composite material consists of at least two chemically different phases, its properties are strongly influenced by a number of factors. One of the most important is the integration of the two phases, which depends on the filler size and size distribution. In order to characterize the morphology and chemical composition of HAP, SEM–EDX imaging was used. Figure 1A shows that the particles exhibited an irregular form. The analysis of particle sizes indicates that the HAP average size was 225 ± 4 nm, a semi-nano range with a narrow size distribution, allowing homogeneous distribution into the composites. It should be noted that previous to ultrasonic treatment, the HAP particle size was 48.6 ± 2 μm, indicating the efficiency of the applied methodology in reducing the particle size. The Ca:P molar ratio (1.67; Figure 1B) was similar to that of cortical bone mineral previously reported (1.64) (Kuhn *et al*., 2008).

DOI: 10.1002/term

m

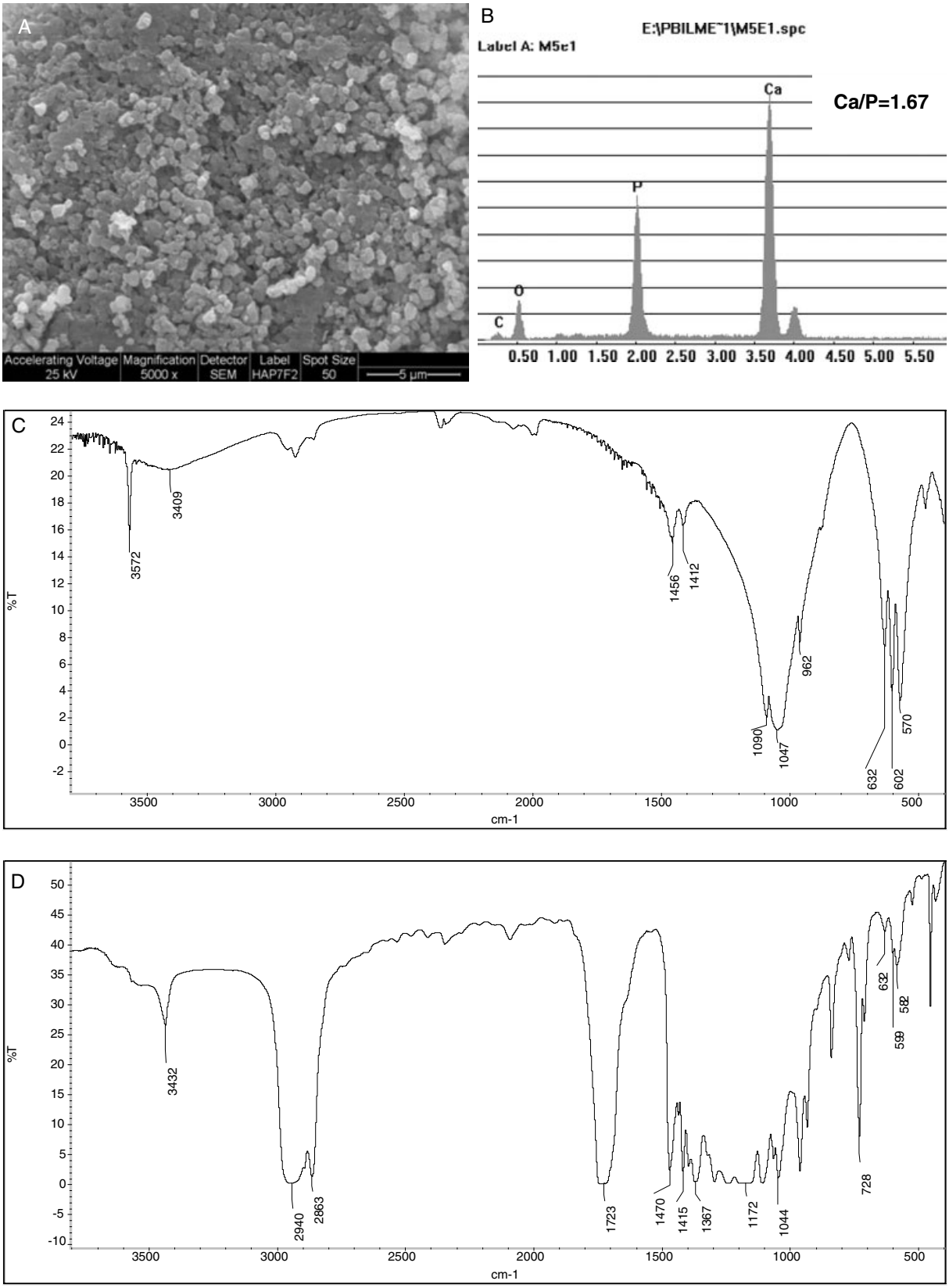

Figure 1. SEM (A), EDX spectra (B), FTIR analysis (C) for HAP, and FTIR of Blend–HAP (D)

DOI: 10.1002/term

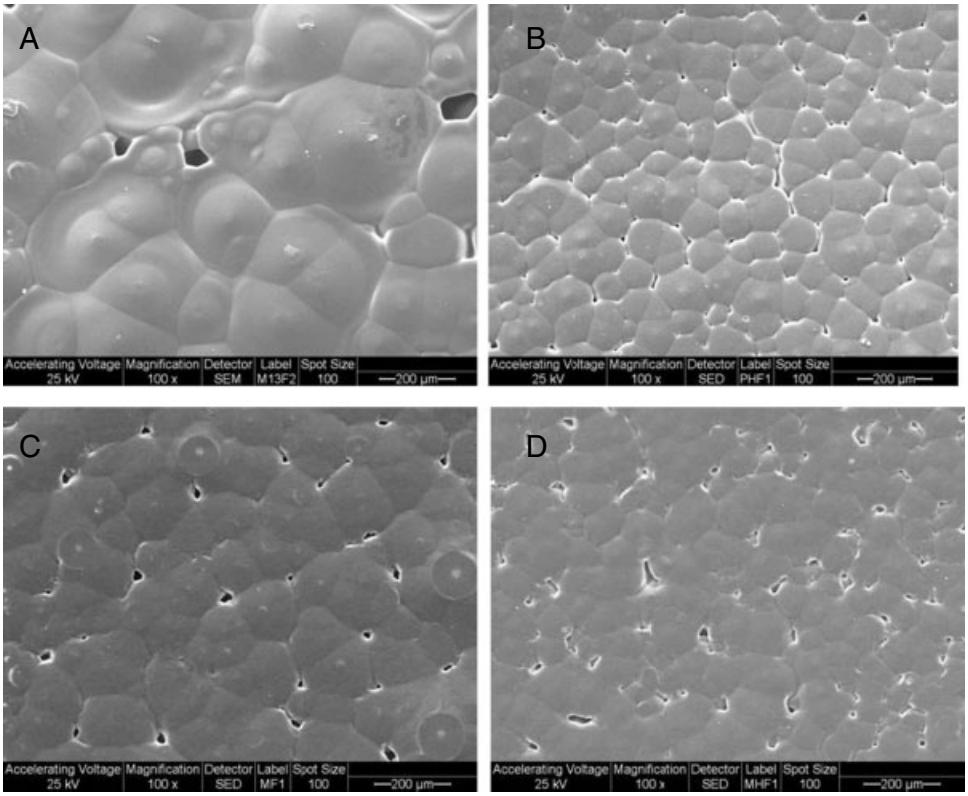

Figure 2. SEM images of the surface of PCL (A), PCL–HAP (B), Blend (C) and Blend–HAP (D)

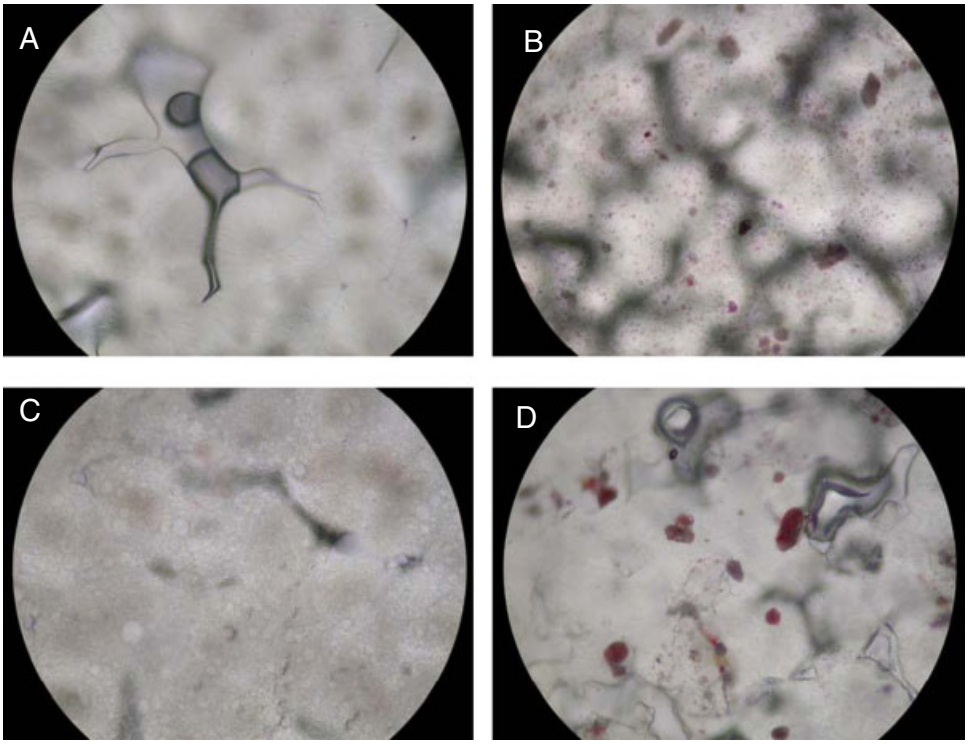

Figure 3. Distribution of HAP in the scaffolds. PCL (A), PCL–HAP (B), Blend (C) and Blend–HAP (D) films were stained with alizarin red S to demonstrate the presence of Ca in HAP incorporated in the films. Original magnification, ×40

DOI: 10.1002/term

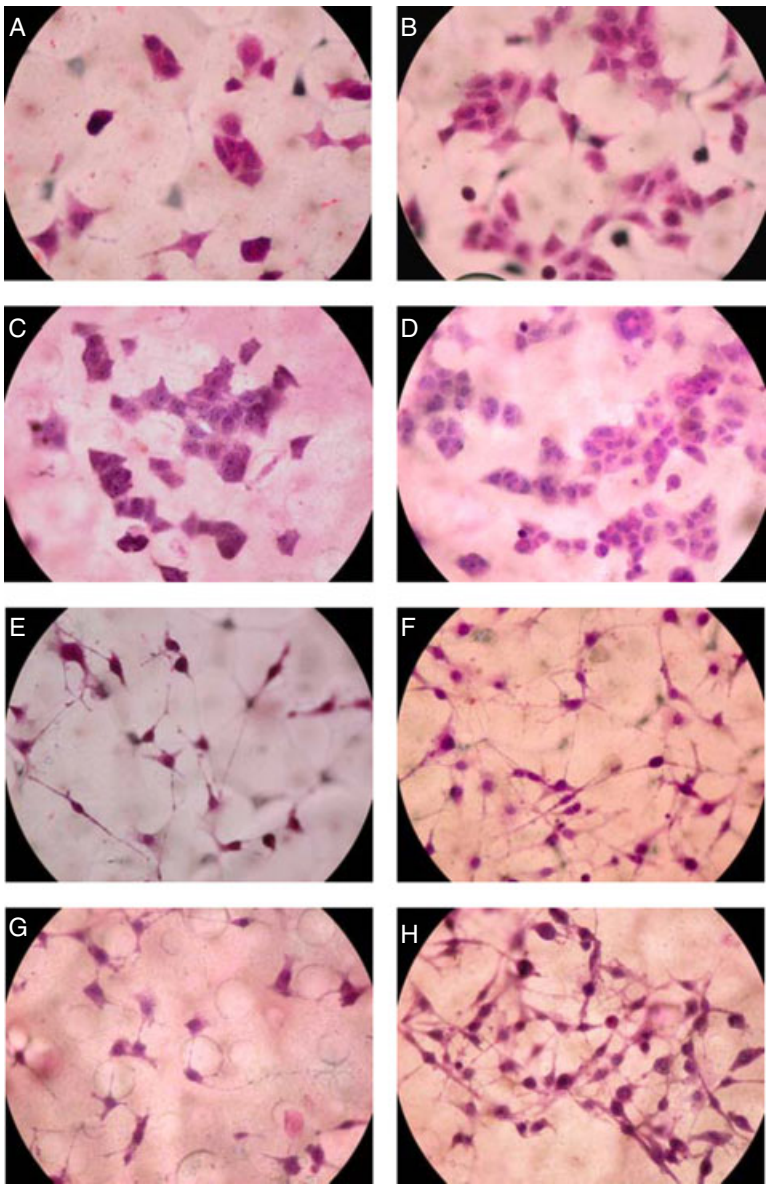

Figure 4. UMR106 (A–D) and MC3T3E1 (E–H) cells growing on different scaffolds. Cells were plated onto PCL (A, E), PCL–HAP (B, F), Blend (C, G) and Blend–HAP (D, H) and cultured for 24 h. After this incubation period the cells were fixed and stained with Giemsa. Original magnification, ×40

The C:P molar ratio (0.03) suggests a few carbonate impurities (1.25g carbonate %HAP). Figure 1C shows the FTIR spectrum of HAP. The bands at 3572, 3409 and 632 cm^{-1} correspond to the structural OH groups (free and associated) in the HAP crystals (Joschek *et al.*, 2000; Walters *et al.*, 1990). The bands at 1090, 1047, 602 and 570 cm^{-1} indicate the presence of a PO_4^{3-} group. In addition, it shows bands at 1456 and 1412 cm^{-1}, corresponding to a CO_3^{2-} component, as shown by EDX analysis. In Blend–HAP (Figure 1D), which contains 1% HAP, characteristic bands of PCL and PFIP were observed, 1723 cm^{-1} (ν C═O), 1172 cm^{-1} (ν C-O), 1470 and 1415 cm^{-1} (ν CH_2). The first two bands appear to be broader in Blend–HAP than that in Blend alone (data not shown), probably accounting for crystallinity changes. An association between HAP and polymers was suggested by observation of the shift in the bands at 1047, 602 and 570 cm^{-1} to 1044, 599 and 582 cm^{-1}, respectively.

Figure 2 shows the microstructure of PCL, PCL–HAP, compatibilized blend, and Blend–HAP. The scaffolds show the typical spherulite-like morphology similar to that previously described for pure PCL. The addition of a small percentage of HAP into the matrix induced a small decrease in the spherulite size. This was also associated with an increased surface roughness for the polymer–HAP.

We also used the alizarin red S staining to observe the aspect and apatite distribution in the films. Figure 3 show homogeneous and fine HAP particle distribution in the PCL–HAP matrix, with patched and stronger-staining HAP particles in the Blend. No staining was found in the control PCL and Blend films.

DOI: 10.1002/term

Table 1. Mechanical properties of PCL and compatibilized PCL–PDIPF blends with or without HAP scaffolds

Scaffold	Elastic modulus (MPa)	Ultimate tensile stress (MPa)	Elongation at breaking point (%)
PCL	161 ± 16	$15.2 \pm 1.7^{**}$	$366 \pm 96^{**}$
PCL–HAP	$249 \pm 12^{*}$	$16.5 \pm 0.5^{**}$	210 ± 21
Blend	143 ± 12	7.7 ± 0.7	60 ± 12
Blend–HAP	$182 \pm 6^{\#}$	7.4 ± 0.7	$20 \pm 1^{\#}$

Results are expressed as mean ± SEM, $n = 8$.
$^{*}p < 0.05$, statistically different from all other groups.
$^{**}p < 0.001$, statistically different compared with Blend and Blend–HAP.
$^{\#}p < 0.05$, statistically different from Blend.

Table 1 shows mechanical properties evaluated for the different scaffolds. The addition of HAP affected the resistance of the PCL and Blend matrices, as evaluated by the elastic modulus. The observed moduli of PCL–HAP and Blend–HAP represent increments of 55% and 27%, respectively, compared to scaffolds without HAP. No changes were observed in the ultimate tensile stress by the addition of apatite to the matrices. However, HAP induced a decrease in the elongation-at-break of PCL (43%) and Blend (67%), a measurement of the ductility of a material. All together these observations suggest that the mechanical properties of the HAP scaffolds were improved significantly.

3.2. Biocompatibility studies

In order to investigate the effect of the addition of HAP on the biocompatibility of scaffolds, two osteoblastic lines were used to study proliferation and differentiation on different matrices. Figure 4 shows the aspect of the UMR106 (A–D) and MC3T3E1 (E–H) cells growing on different scaffolds for 24 h. In general the cells adhered and proliferated well, developing extensions and spreading on all matrices. However, the addition of 1% HAP in the PCL and Blend increased cell proliferation. These observations were further confirmed by quantification of the number of growing cells after 24 h, and are presented in Figure 5A (UMR106) and 5B (MC3T3E1). It was also observed, as we have previously described (Fernandez *et al*., 2010), that UMR106 but not MC3T3E1 cells proliferated better in the blend when compared with the PCL film (Figure 5A). Nevertheless, both cell lines seemed to prefer the polymer–HAP scaffolds.

We also evaluated the capacity of cells growing on different matrices to express two markers of bone formation. Figure 6A, C shows the expression of ALP after culturing osteoblasts for 48 h (UMR106) or 2 weeks (MC3T3E1). In the case of the osteosarcoma line (Figure 6A), the addition of HAP induced a slight increase in ALP expression. In contrast, the apatite significantly inhibited ALP expression when MC3T3E1

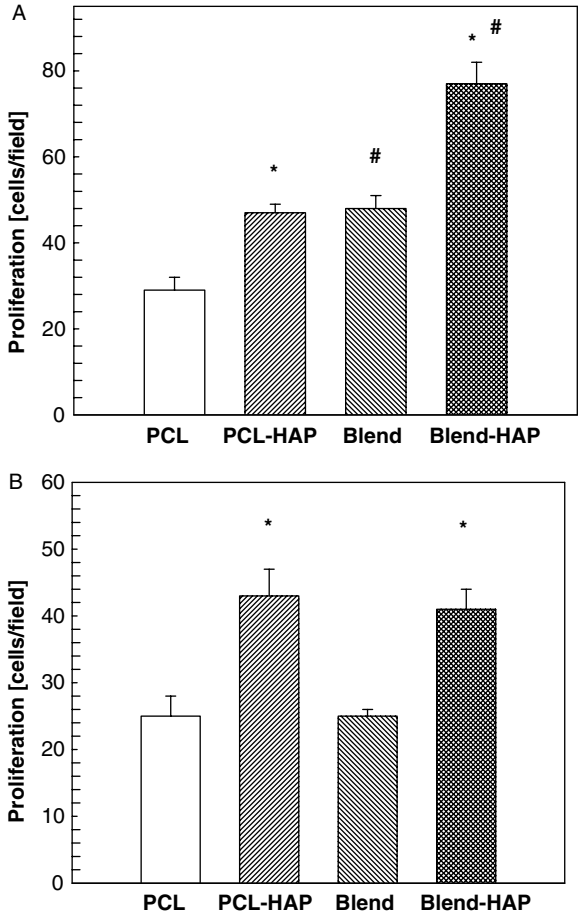

Figure 5. UMR106 (A) and MC3T3E1 (B) proliferation after 24 h culture on PCL, PCL–HAP, Blend or Blend–HAP. Quantitation was assessed by counting the number of cells per field in 10 representative fields per scaffold. Values are shown as mean ± SEM. $^{*}p < 0.05$ **vs. scaffold without HAP;** $^{\#}p < 0.05$ **vs. PCL**

cells (Figure 6C) were induced to differentiate in an osteogenic medium for 2 weeks. The production of type I collagen, the main extracellular matrix protein expressed in bone, was also evaluated. As can be seen in Figure 6B, HAP significantly increased the production of collagen in both types of scaffold, the PCL and the Blend. When MC3T3E1 cells were cultured for 2 weeks in an osteogenic medium, the addition of HAP only stimulated collagen production in the Blend (Figure 6D).

3.3. Effects of scaffolds on osteoblastic transcription factor Runx2

We next evaluated the effect of different matrices on the expression of one of the major transcription factors for osteoblastogenesis, Cbfa1/Runx2. MC3T3E1 cells growing on different scaffolds were cultured in an osteogenic medium for 3 weeks. Western immunoblot analysis showed that when compared with cells cultured in PCL or Blend, MC3T3E1 in the polymer–HAP scaffolds expressed significantly more Runx2 (Figure 7).

DOI: 10.1002/term

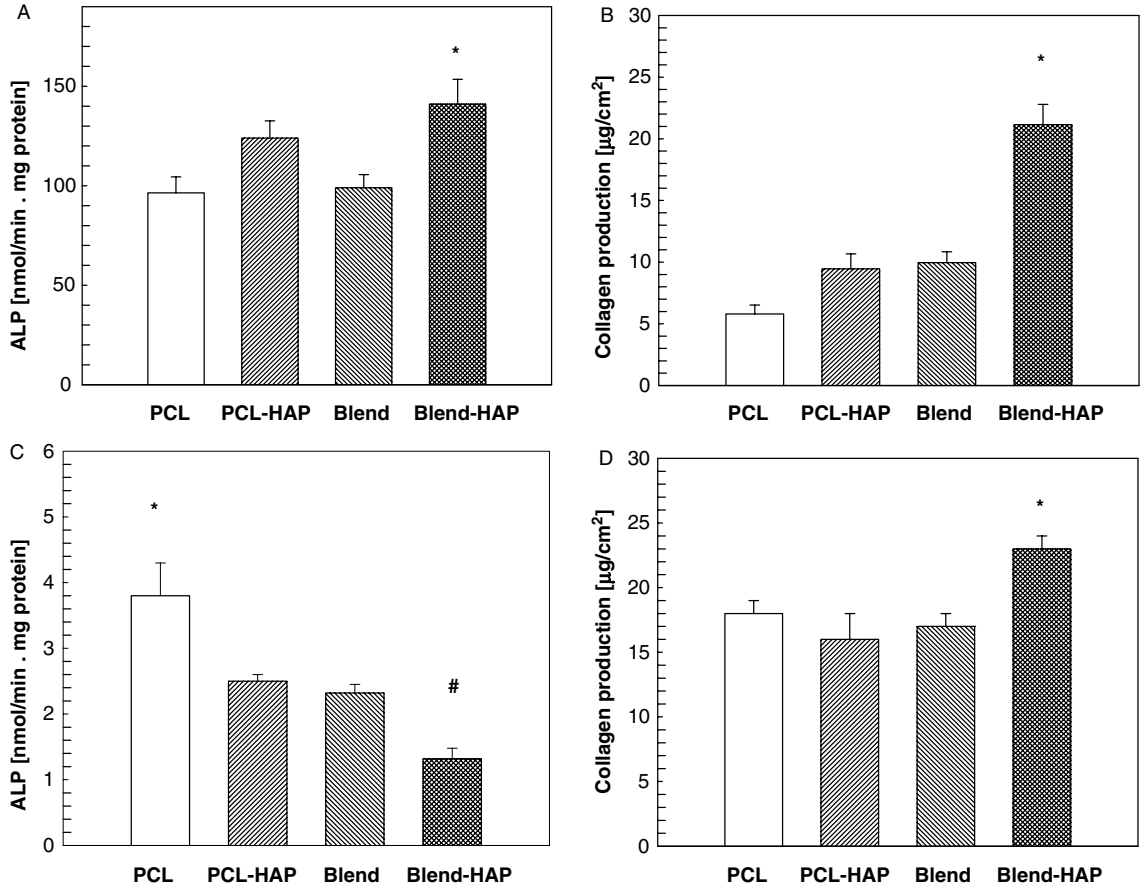

Figure 6. Effect of the scaffolds on the expression of osteoblastic markers. UMR106 (A, B) and MC3T3E1 (C, D) were cultured on different scaffolds for 48 h or 2 weeks, respectively. ALP (A, D) and type-I collagen production (B, D) were evaluated as described in Materials and methods. Values are shown as mean ± SEM. $^{*}p < 0.05$ **vs. all other groups;** $^{\#}p < 0.05$ **vs. Blend**

4. Discussion

We have previously shown that ultrasound-compatibilized PCL–PDIPF blends exhibit better biocompatibility with UMR106 and MC3T3E1 osteoblastic cells than homopolymers (PCL and PDIPF) and the physical blend (Fernandez *et al.*, 2010). It has been recognized that scaffolds that will act as temporary matrices for cell proliferation and extracellular matrix deposition, with consequent bone in-growth until the new tissue is totally restored or regenerated, must have a series of essential properties (Salgado *et al.*, 2004). In addition to biocompatibility, porosity and osteoinductivity in order to promote cellular adhesion and growth, is also crucial that these materials have mechanical properties similar to native bone. To achieve this goal, different polymer–HAP composites have been studied, and improved mechanical properties have been demonstrated. The present study describes the design of a new scaffold for bone tissue engineering based on compatibilized PCL–PDIPF blends which incorporate HAP in order to enhance their properties.

Our results demonstrate that the irregular form of the obtained HAP interacted adequately with the polymer because, as has been indicated, it forms a mechanical interlock with the particle (Šupová, 2009). In relation to the particle size of HAP, some investigators have shown a significant increase in cell adhesion and proliferation in nano-sized HAP (<100 nm) as a component of HAP–polymer composites (Webster *et al.*, 2000; Li *et al.*,

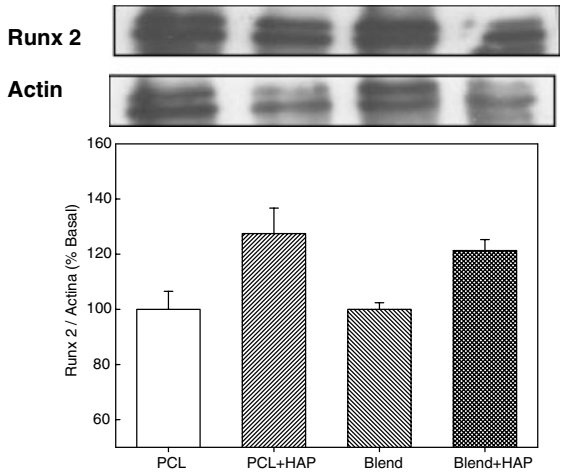

Figure 7. Effect of the scaffolds on the expression of Runx-2 in MC3T3E1 cells. Cells were plated on different scaffolds and cultured in an osteogenic medium for 2 weeks. The expression of Runx-2 and actin was evaluated by western immunoblot. The blots were quantified using the Scion-β2 image program and the corresponding values are shown as bar graphs. Values are expressed as mean ± SEM

DOI: 10.1002/term

2009). It has been shown that nano-HAP crystals, due to their surface characteristics, have a stronger capability to absorb certain proteins that promote cell adhesion. Although our HAP has a size in the nm range (225 nm), its morphology and good interphase compatibility in the composite (evaluated by FTIR) suggest promissory results.

Another important aspect we have considered is the distribution of HAP inside the composite. Alizarin red staining shown an appropriate distribution of particles which ensures that the composite exhibits isotropic properties.

Important requirements for scaffold materials are their mechanical properties, considering that as temporary bone substitutes they must encourage repair by providing mechanical support until the tissue is regenerated and remodelling occurs naturally (Prabhakaran *et al*., 2009). Our results show that the HAP–polymer composites exhibit an increase in the elastic modulus in comparison to polymer (PCL or blend), which demonstrates that HAP inclusion improves their mechanical properties. The ultimate tensile stress of HAP–Blend composite was very similar to that of mouse femur (about 10 MP) (Ding *et al*., 2010), showing significant differences with respect to PCL–HAP. The decrease in the elongation-at-break induced by HAP on PCL and Blend suggests that the obtained composite is less ductile. Both the higher elastic modulus and lower strain at failure of HAP–polymer composite can be explained by the stiffness and plasticity in deformation produced by the HAP mineral, which is typical of hard inorganic phases.

In the present study we have evaluated different parameters in order to assess the biocompatibility/cytotoxicity of the scaffolds for two osteoblastic lines. We have found that the addition of HAP to both PCL and Blend significantly improves the biocompatibility and osteogenicity of the scaffolds. Evidence for this notion is based in several observations: (a) HAP–polymer increases proliferation of osteoblastic cells; (b) HAP included in the blend increases ALP expression in UMR106 cells; (c) HAP–Blend increases the type I collagen production in both cell lines; and (d) higher levels of the osteogenic transcription factor Runx-2 were detected when MC3T3E1 osteoblasts were induced to differentiate and mineralize on HAP–polymer scaffolds. These observations indicate that the incorporation of hydroxyapatite increases the *in vitro* osteogenicity of PCL and Blend films.

Previously we have developed a compatibilized blend that was able to support the growth and differentiation of osteoblasts better than homopolymers. The present study extends those observations and demonstrates that there is a further advantage for HAP–polymer to support the proliferation of osteoblasts. Other authors have already proposed HAP–PCL composites for bone engineering. For instance, Choi *et al*. (2004) prepared a HAP–PCL composite using a synthetic apatite that was included at 10–40 wt% in the polymer. This material was suggested to be suitable as a bone substitute scaffold, although the authors did not investigate its biocompatibility/osteoinduction properties. In addition, Kim *et al*. (2004) developed a HAP–PCL composite porous bone scaffold for drug delivery. Recently Scaglione *et al*. (2009) designed and developed a 3D osteoconductive polymeric-based wide-net mesh using PCL and HAP. They showed that the scaffolds displayed preferential cell adhesion to the fibres with HAP in comparison with the pure PCL fibre, as well as better *in vivo* bone ingrowth and blood vessel colonization. Thus, our present composite has the advantage of using a previously characterized polymer (PCL) as well as PDIPF. This polyfumarate is a more brittle material with a high tensile strength which, when compatibilized with PCL, gives rise to a material with better mechanical properties. The addition of HAP to the Blend further improves its mechanical properties and osteoinductive capability, strengthening its use as a substrate for hard tissue replacement.

Our present results also show that HAP–Blend improved the surface available for osteoblastic differentiation, mineralization and expression of osteogenic transcription factors, which are crucial for bone formation. Since the scaffold material contains Ca/P–apatite, it was not possible to evaluate mineralization (Ca/P deposition) into the matrix by classic techniques such as Sirius red S (for Ca) or von Kossa (for P) staining. Thus, we evaluated the expression of Runx-2, one of the major transcription factors expressed during osteogenesis. After 3 weeks (mineralization period) of culture in an osteogenic medium, the pre-osteoblastic MC3T3E1 cell line was committed to differentiate and mineralize the matrix, and Runx-2 was expressed strongly when cells were grown on HAP–polymer scaffolds.

5. Conclusions

We synthesized a novel scaffold, a PCL–PDIPF blend incorporating hydroxyapatite composite (HAP–Blend), a material with uniform dispersion of semi-nano HAP particles and good interphase compatibility. The physical, mechanical and biological properties of the scaffold were compared with those of a Blend and PCL without apatite. The inclusion of HAP substantially improves the mechanical properties of the Blend. The *in vitro* cell culture experiments suggest that the new HAP–Blend was more osteogenic than the blend or PCL scaffolds. Together the results suggest that the developed HAP–Blend composite may potentially be used in bone tissue-engineering applications.

Acknowledgements

This work was partially supported by grants from Facultad de Ciencias Exactas, Universidad Nacional de La Plata (UNLP), Comisión de Investigaciones Científicas de la Provincia de Buenos Aires (CICPBA) and Agencia Nacional de Ciencia y Tecnologia (ANPCYT; Grant Nos BID-1728/OC-AR and PAE 22398) to A.M.C. J.M.F. is a fellow of CONICET; M.S.M. is a member of the Carrera del Investigador (CONICET); A.M.C. is a member of the Carrera del Investigador (CICPBA); and MSC is a Professor at UNLP.

References

Bradford MM. 1976; A rapid and sensitive method for the quantitation of microgram quantities of protein utilizing the principle of protein–dye binding. *Anal Biochem* **72:** 248–254.

Choi D, Marra KG, Kumta PN. 2004; Chemical synthesis of hydroxyapatite/poly(ε-caprolactone) composites. *Mat Res Bull* **39:** 417–432.

Cortizo AM, Molinuevo MS, Barrio DA, *et al*. 2006; Osteogenic activity of vanadyl(IV)–ascorbate complex: evaluation of its mechanisms of action. *Int J Biochem Cell Biol* **38:** 1171–1180.

Cortizo MS. 2007; Polymerization of diisopropyl fumarate under microwave irradiation. *J Appl Polym Sci* **103:** 3785–3791.

Cortizo MS, Molinuevo MS, Cortizo AM. 2008; Biocompatibility and biodegradation of polyester and polyfumarate based-scaffolds for bone tissue engineering. *J Tissue Eng Regen Med* **2:** 33–42.

Ding WG, Jiang SD, Zhang YH, *et al*. 2010; Bone loss and impaired fracture healing in spinal cord injured mice. *Osteoporos Int* (DOI: 10.1007/s00198–010–1256–8).

Fernandez JM, Molinuelo MS, Cortizo AM, *et al*. 2010; Characterization of poly-ε-caprolactone/polyfumarate blends as scaffolds for bone tissue engineering. *J Biomat Sci Polym Ed* **21:** 1297–1312.

Habibovic P, de Groot K, 2007; Osteoinductive biomaterials – properties and relevance in bone repair. *J Tissue Eng Regen Med* **1:** 25–32.

Joschek S, Nies B, Krotz R, *et al*. 2000; Chemical and physicochemical characterization of porous hydroxyapatite ceramics made of natural bone. *Biomaterials* **21:** 1645–1658.

Kim HW, Knowles JC, Kim HE. 2004; Hydroxyapatite/poly(ε-caprolactone) composite coatings on hydroxyapatite porous bone scaffold for drug delivery. *Biomaterials* **25:** 1279–1287.

Kim SS, Park MSA, Jeon O, *et al*. 2006; Poly(lactide-co-glycolide)/hydroxyapatite composite scaffolds for bone tissue engineering. *Biomaterials* **27:** 1399–1409.

Kuhn LT, Grynpas MD, Rey CC, *et al*. 2008; A comparison of the physical and chemical differences between cancellous and cortical bovine bone mineral at two ages. *Calcif Tissue Int* **83:** 146–154.

Laemmli UK. 1970; Cleavage of structural protein during the assembly of the head of bacteriophage T4. *Nature* **227:** 680–685.

Li J, Dou Y, Yang J, *et al*. 2009; Surface characterization and biocompatibility of micro- and nano-hydroxyapatite/chitosan–gelatin network films. *Mat Sci Eng C-Bio S* **29:** 1207–1215.

Mano JF, Silva GA, Azevedo HS, *et al*. 2007; Natural origin biodegradable systems in tissue engineering and regenerative medicine: present status and some moving trends. *J R Soc Interface* **4:** 999–1030.

McCarthy AD, Etcheverry SB, Bruzzone L, *et al*. 1997; Effects of advanced glycation end-products on the proliferation and differentiation of osteoblast-like cells. *Mol Cell Biochem* **170:** 43–51.

Molinuevo MS, Schurman L, McCarthy AD, *et al*. 2010; C. Effect of Metformin on bone marrow progenitor cell differentiation: *in vivo* and *in vitro* studies. *J Bone Miner Res* **25:** 211–221.

Ooi CY, Uamdi MH, Ramesh S. 2007; Properties of hydroxyapatite produced by annealing of bovine bone. *Ceram Int* **33:** 1171–1177.

Partridge NC, Alcorn D, Michelangeli VP, *et al*. 1983; Morphological and biochemical characterization of four clonal osteogenic sarcoma cell lines of rat origin. *Cancer Res* **43:** 4308–4314.

Prabhakaran MP, Venugopal J, Ramakrishna S. 2009; Electrospun nanostructured scaffols for bone tissue engineering. *Acta Biomater* **5:** 2884–2893.

Quarles LD, Yahay DA, Lever LW, *et al*. 1992; Distinct proliferative and differentiated stages of murine MC3T3E1 cells in culture: an *in vitro* model of osteoblast development. *J Bone Miner Res* **7:** 683–692.

Salgado AJ, Coutinho OP, Reis RL. 2004; Bone tissue engineering: state of the art and future trends. *Macromol Biosci* **4:** 743–765.

Scaglione S, Ilengo C, Fato M, *et al*. 2009; Hydroxyapatite-coated polycaprolactone wide mesh as a model of open structure for bone regeneration. *Tissue Eng Part A* **15:** 155–163.

Šupová M. 2009; Problem of hydroxyapatite dispersion in polymer matrices: a review. *J Mater Sci: Mater Med* **20:** 1201–1213.

Tullberg-Reinert H, Jundt G. 1999; *In situ* measurement of collagen synthesis by human bone cells with a Sirius red-based colorimetric microassay: effects of transforming growth factor β2 and ascorbic acid 2-phosphate. *Histochem Cell Biol* **112:** 271–276.

Walters MA, Leung YC, Blumenthal NC, *et al*. 1990; A Raman and infrared spectroscopic investigation of biological hydroxyapatite. *J Inorg Biochem* **39:** 193–200.

Wang M. 2003; Developing bioactive composite materials for tissue replacement. *Biomaterials* **24:** 2133–2151.

Webster TJ, Ergun C, Doremus RH, *et al*. 2000; Specific proteins mediate enhanced osteoblast adhesion on nanophase ceramics. *J Biomed Mater Res* **51:** 475–483.